VOL. 7, NO. 3, MARCH 2012 ISSN 1819-6608
ARPN Journal of Engineering and Applied Sciences


www.arpnjournals.com

PSEUDOTIME APPLICATION TO HYDRAULICALLY FRACTURED VERTICAL GAS WELLS AND HETEROGENOUS GASRESERVOIRS USING THE TDS TECHNIQUE

Freddy Humberto Escobar, Laura Yissed Martinez, Leidy Johanna Mendez and Luis Fernando Bonilla
Universidad Surcolombiana, Av. Pastrana - Cra. 1, Neiva (Huila-Colombia)
E-Mail: fescobar@usco.edu.co

ABSTRACT

Contrary to liquid flow, the viscosity and compressibility of gases change substantially as pressure varies. This phenomenon has to be carefully modeled, so the gas flow equation can be adequately linearized to allow for the liquid diffusivity solution to satisfy gas behavior when analyzing gas transient test data. The first solution to this problem was the introduction of the pseudopressure function that responds for variations of viscosity, density and compressibility which are combined into a single variable called "pseudopressure". Since, the dimensionless time function is also sensitive to changes in both viscosity and compressibility of gases, then, the pseudotime function was incorporated to combine these simultaneous variations into a single variable. This makes more accurate the estimation of the reservoir parameters. A recent study using the *TDS* technique has found little differences in estimation of permeability, wellbore storage coefficient and skin factor using either pseudotime or real time. However, the estimation of the drainage area is better determined when using pseudotime. This paper has the objective of extending the *TDS* technique for hydraulically fractured gas wells and heterogeneous gas formations and conducting a comparative study in the estimation of both the half-length and conductivity of a vertical fracture and the naturally fractured reservoir parameters. The new relationships were successfully tested on synthetic and actual field data. It was found better results when using the pseudotime function.

Keywords: pressure test, gas reservoirs, hydraulic fractures, *TDS* technique, pseudotime, reservoirs naturally fractured.

RESUMEN

Contrario al flujo de gas, la viscosidad y compresibilidad de los gases cambian substancialmente a medida que la presión varía. Este fenómeno debe ser cuidadosamente modelado de modo que la ecuación de flujo gaseoso se puede linealizar adecuadamente para permitir que la solución de difusividad líquida satisfaga el comportamiento de los gases cuando se analizan pruebas transitorias de presión en yacimientos gasíferos. La primera solución a este problema se hizo con la introducción de la función pseudopresión que responde por las variaciones de viscosidad, densidad y compresibilidad las cuales se combinan en una variable sencilla "pseudopresión". Puesto, que la función de tiempo adimensional es también sensible a cambios de viscosidad y compresibilidad de los gases, entonces, se incorporó la función de pseudotiempo para combinar estas variaciones simultáneas en una única variable. Con esto se mejora la exactitud en la estimación de los parámetros del yacimiento.

Un estudio reciente que usa la técnica *TDS* encontró pocas diferencias en los cálculos de permeabilidad, coeficiente de almacenamiento y daño cuando se usa pseudotiempo o tiempo real. Sin embargo, el área de drenaje se estima con mayor exactitud usando el pseudotiempo.

Este artículo tiene como objeto extender la técnica *TDS* para pozos de gas hidráulicamente fracturados y yacimientos de gas heterogéneos y de conducir un estudio comparativo en la estimación la longitud y conductividad de una fractura hidráulica, así como los parámetros de los yacimientos naturalmente fracturados. Las nuevas expresiones se aplicaron satisfactoriamente a casos reales y sintéticos. Se encontraron mejores resultados cuando se usa la function de pseudotiempo.

Palabras clave

pruebas de presión; yacimientos de gas; técnica *TDS*; pseudotiempo; fracturas hidráulicas; yacimientos naturalmente fracturados.

1. INTRODUCTION

On one hand, gas well testing ought to have a careful treatment since such important properties as viscosity; density and compressibility cannot be considered to stay constant during a pressure test. To overcome this issue, Al-Hussainy (1966) introduced a very important concept to include the variation of the above mention parameters into a single function. This was called the pseudopressure function which has become the most accurate tool for gas well test interpretation. On the other hand, the dimensionless time function also includes viscosity and compressibility which are very sensitive in gas systems. Conventionally, this function is estimated with the initial constant value of such properties which is a conceptual error. This problem was also solved by Agarwal (1979) who developed the pseudotime function to combine the simultaneous changes of gas viscosity and system compressibility, and performed practical applications to pressure buildup tests in vertical fractured wells. Just to name a couple of important applications of this concept, Lee and Holditch (1982) demonstrated the advantages of using the pseudotime function in pressure buildup testing of tight formations and Spivey and Lee (1986) applied the pseudotime function to linearize the gas governing equation under prevalent conditions of wellbore

storage during interpretation of pressure buildup tests and to use both pseudotime and pseudopressure for drawdown cases.

Nunez *et al*. (2002) and (2003) applied the pseudopressure function to homogeneous reservoir and fractured vertical wells to gas reservoir using the *TDS* technique. For comparison purposes computations with actual time and pseudotime, Escobar *et al*. (2007), using the *TDS* technique, found differences in the determination of the reservoir drainage area. However, practically no impact was found on the determination of permeability, wellbore storage coefficient and skin factor.

2. MATHEMATICAL FORMULATION

2.1 Fractured wells

The system under consideration is assumed to possess a fully-penetrating vertical hydraulic fracture well which has a half length, x_f, width, w_f, and permeability, k_f. Reservoir porosity and permeability are constant, and no wellbore storage effects are considered. The dimensionless parameters are defined as:

$$t_{DaA} = \left(\frac{0.0002637k}{\phi A} \right) t_a(P) \tag{1}$$

$$m(P)_D = \frac{kh\left(m(P_i) - m(P)\right)}{1422.52 q_{sc} T} \tag{2}$$

$$\left(t_{DaA} * m(P)'_D\right) = \frac{kh\left(t_a(P) * \Delta m(P)'\right)}{1422.52 q_{sc} T} \tag{3}$$

Escobar *et al*. (2007) developed the equations for permeability and skin factor including pseudotime:

$$k = \frac{711.26 q_{sc} T}{h\left(t_a(P) * \Delta m(P)'\right)_r} \tag{4}$$

$$s' = 0.5\left[\frac{\Delta m(P)_r}{\left(t_a(P) * \Delta m(P)'\right)_r} - \ln\left(\frac{k t_a(P)_r}{\phi r_w^{\,2}} \right) + 7.43 \right] \tag{5}$$

2.1.1 Uniform flux fracture

At early times, the reservoir flow towards the fracture is linear. The duration of this flow is a function of the ratio x_e/x_f. The governing dimensionless pressure and pressure derivative equations for this flow are:

$$m(P)_D = 3.544 \left(\frac{x_e}{x_f} \right) \sqrt{t_{DaA}} \tag{6}$$

$$\left(t_{DaA} * m(P)'_D\right)_L = 1.772 \left(\frac{x_e}{x_f} \right) \sqrt{t_{DaA}} \tag{7}$$

After plugging the dimensionless quantities, Eqs. 1 and 3, into Eqs. 6 and 7, expressions to obtain half-fracture length as a function of either pseudopressure or pseudopressure derivative read at the pseudotime of 1 hr are given as:

$$x_f = \frac{40.944 q_{sc} T}{h\left(\Delta m(P)\right)_{L1} \sqrt{\phi k}} \tag{8}$$

$$x_f = \frac{20.472 q_{sc} T}{h\left(t_a(P) * \Delta m(P)'\right)_{L1} \sqrt{\phi k}} \tag{9}$$

The governing equation during the late pseudosteady-state regime is given by:

$$\left(t_{DaA} * m(P)'_D\right) = 2\pi t_{DaA} \tag{10}$$

From Eq. 10, an expression is found to obtain reservoir drainage area from an arbitrary pressure derivative point during pseudosteady state:

$$A = \frac{2.357 q_{sc} T t_a(P)_{pss}}{\phi h \left(t_a(P) * \Delta m(P)'\right)_{pss}} \tag{11}$$

The uniform-flux behavior during late pseudosteady-state regime is governed by:

$$m(P)_D = 2\pi t_{DaA} + \ln\left(x_e / x_f\right) + \ln\sqrt{\frac{2.2458}{C_A}} \tag{12}$$

Combination of the derivative of Eq. 12 with Eq. 10 allows for developing an expression to estimate the Dietz´s shape factor:

$$C_A = 2.2458 \left(\frac{x_e}{x_f} \right)^2 \exp\left[\left(1 - \frac{\Delta m(P)_{pss}}{\left(t_a(P) * \Delta m(P)'\right)_{pss}} \right) \frac{0.0003313 k t_a(P)_{pss}}{\phi A} \right] \tag{13}$$

During radial flow regime, the dimensionless pressure derivative takes the value of one half; therefore, we obtain from Eqs. 7 and 10 the following relationships, respectively:

$$\frac{x_f^2}{k} = \frac{t_a(P)_{rLi}}{1207.09\phi} \tag{14}$$

$$A = \frac{k t_a(P)_{rpi}}{301.772\phi} \tag{15}$$

The intersection point of the straight lines from Eqs. 7 and 10 also leads to obtain an alternative form of estimating the half-fracture length:

$$k x_f^2 = \frac{75.443 \phi A^2}{t_a(P)_{Lpi}} \tag{16}$$

2.1.2 Infinite-conductivity fractures

The governing dimensionless pressure derivative equation presented by Tiab (1994) during bi-radial flow applied to gas systems is given by:

$$\left(t_{DaA} * m(P)'_D\right) = 0.769\left(\frac{x_e}{x_f}\right)^{0.72} t_{DaA}^{0.36} \quad (17)$$

From integration of Eq. 17, it yields,

$$m(P)_D = 2.1361\left(\frac{x_e}{x_f}\right)^{0.72} t_{DaA}^{0.36} \quad (18)$$

Once the dimensionless quantities are replaced into Eqs. 17 and 18 and solving for the half-fracture length the following equations are obtained:

$$x_f = 0.694 x_e \left[\frac{G_{BR}}{\left(t_a(P) * \Delta m(P)'\right)_{BR1}}\right]^{1.388} \quad (19)$$

$$x_f = 2.8695 x_e \left[\frac{G_{BR}}{\Delta m(P)_{BR1}}\right]^{1.388} \quad (20)$$

Being:

$$G_{BR} = \frac{73.224 q_{sc} T}{kh}\left(\frac{k}{\phi A}\right)^{0.36} \quad (21)$$

An expression to find reservoir permeability is found from combining Eqs. 7 and 17:

$$k = 128.051 \frac{q_{sc} T}{h\left(t_a(P) * \Delta m(P)'\right)_{L1}}\left(\frac{1}{t_a(P)_{BRLi}^{0.5}}\right) \quad (22)$$

Eq. 17 is set equal to 0.5 during radial flow regime. This corresponds at the intersection point of the radial and bi-redial lines. Then, the following equation is derived:

$$\frac{x_f^2}{k} = \frac{t_a(P)_{rBRi}}{4587.03\phi} \quad (23)$$

The intersection point of the bi-radial and late pseudosteady-state lines, Eqs. 17 and 10 leads to another expression to find reservoir permeability:

$$k = \frac{142.20\phi A}{t_a(P)_{BRpi}}\left(\frac{x_e}{x_f}\right)^{1.125} \quad (24)$$

2.1.3 Finite-conductivity fractures

The governing dimensionless pressure derivative equation during bilinear flow regime is expressed by:

$$m(P)_D = \left(\frac{2.451}{\sqrt{C_{fD}}}\right) t_{Daxf}^{0.25} \quad (25)$$

$$\left(t_{Daxf} * m'(P)_D\right) = \left(\frac{0.6127}{\sqrt{C_{fD}}}\right) t_{Daxf}^{0.25} \quad (26)$$

The mathematical definition of dimensionless fracture conductivity as presented by Cinco-Ley *et al*. (1979) is:

$$C_{fD} = \left(\frac{k_f}{k}\right)\left(\frac{w_f}{x_f}\right) \quad (27)$$

The apparent fracture conductivity is obtained from Eq. 25 and 26 when both the pseudopressure and pseudopressure derivative are read at a pseduotime value of 1 hr:

$$\left(k_f w_f\right)_{app} = \frac{197402.4}{\sqrt{\phi k}}\left(\frac{q_{sc} T}{h\left(\Delta m(P)\right)_{BL1}}\right)^2 \quad (29)$$

$$\left(k_f w_f\right)_{app} = \frac{12337.65}{\sqrt{\phi k}}\left(\frac{q_{sc} T}{h\left(t_a(P) * \Delta m(P)'\right)_{BL1}}\right)^2 \quad (30)$$

It is recommended to follow the procedure outlined by Guppy *et al*. (1081) to properly estimate fracture conductivity in either pressure drawdown or buildup by estimating:

$$a = \frac{(C_{fD})_{app_1}}{(C_{fD})_{app_2}} \quad (31)$$

$$(C_{fD})_t = (C_{fD})_{app_2} * \frac{q_2 - q_1}{q_2 - q_1 * a} * a \quad (32)$$

The linear flow regime expression defined by Tiab (1994) can also extended to pseudopressure and pseudotime as:

$$\Delta m(P) = m_L \sqrt{t_a(P)} \quad (33)$$

$$\left(t_a(P) * \Delta m'(P)\right) = 0.5 m_L \sqrt{t_a(P)} \quad (34)$$

Where,

$$m_L = 40.915\left(\frac{q_{sc} T}{h}\right)\sqrt{\frac{1}{\phi k x_f^2}} \quad (35)$$

The intersection of the derivative Eq. 33 with the dimensional form of Eq. 25 allows obtaining:

$$k = \left(\frac{k_f w_f}{x_f^2}\right)^2 \frac{16 t_a(P)_{BLLi}}{13905.12\phi} \quad (36)$$

When Eq. 26 is set equal to 0.5 (intersection of radial and bilinear flow lines), the following expression is derived:

$$t_a(P)_{rBLi} = 1678.85 \frac{\phi}{k^3}\left(k_f w_f\right)^2 \quad (37)$$

Eqs. 8 and 9 are also applied when formation linear flow is observed.

2.1.4 Other relationships

Some relationships can be found from the intersection of the straight lines resulting from the different flow regimes by means of Eqs. 10, 12 and 14.

$$\frac{t_a(P)_{rLi}}{t_a(P)_{rpi}} = \frac{t_a(P)_{rpi}}{t_a(P)_{Lpi}} = \left(\frac{t_a(P)_{rLi}}{t_a(P)_{Lpi}}\right) = \left(\frac{x_f}{x_e}\right)^2 \quad (38)$$

Tiab (2003) developed the following equations which relate the half-fracture length, formation permeability, fracture conductivity and post-frac skin factor:

$$x_f = \frac{1.92123}{\frac{e^s}{r_w} - \frac{3.31739k}{k_f w_f}} \quad (39)$$

Or,

$$k_f w_f = \frac{3.31739k}{\frac{e^s}{r_w} - \frac{1.92123}{x_f}} \quad (40)$$

For short tests such as in low permeability formations, the radial flow regime may unobserved; Tiab (2003) proposed the following expressions:

$$s = \ln\left[r_w\left(\frac{1.92173}{x_f} - \frac{3.31739k}{w_f k_f}\right)\right] \quad (41)$$

The post-frac pseudo skin factor can be evaluated from the following expression introduced by Cinco-Ley *et al*. (1976):

$$s = \ln\frac{r_w}{x_f} + \frac{1.65 - 0.32u + 0.11u^2}{1 + 0.18u + 0.064u^2 + 0.005u^3} \quad (42)$$

Where,

$$u = \ln\left(\frac{w_f k_f}{x_f k}\right) \quad (43)$$

2.2 Double-porosity systems

Extending the concept of Engler and Tiab (1996), the pseudopressure derivative can also be set to zero at the trough; an analytical expression to find the interporosity flow parameter can be obtained from the time at the minimum point:

$$(t_{Da})_{\min} = \frac{\omega}{\lambda}\ln\frac{1}{\omega} \quad (44)$$

An expression to find the interporosity flow parameter was found by Tiab and Escobar (2003) and is extended here after replacing the dimensionless pseudotime function into Eq. 34.

$$\lambda = \frac{3792.2(\phi)_{f+m}\omega r_w^2}{k_{fb}\Delta t_a(P)_{\min}}\left[\omega\ln\left(\frac{1}{\omega}\right)\right] \quad (45)$$

Engler and Tiab (1996) also found a relationship by plotting the dimensionless time against λ which is extended here,

$$\lambda = \frac{1}{(t_{Da})_{us,i}} \quad (46)$$

In field units becomes:

$$\lambda = \left(\frac{\phi r_w^2}{0.0002637k}\right)\frac{1}{[t_a(P)]_{us,i}} \quad (47)$$

The effect of the wellbore storage coefficient on the minimum point was widely studied by Engler and Tiab (1996) and extended to gas wells by Escobar *et al*. (2004) which can be applied to this case and are not reported for space reasons.

Several correlations are presented to find the dimensionless storage coefficient. The ratio between pseudo pressure derivatives at the trough and the radial flow regime allows developing a correlation for $0.01 \le \omega \le 0.1$within an error lower than 3%.

$$\omega = 0.053833\exp\frac{x_1}{0.30499673} - 0.05681 \quad (48)$$

Other correlations, with a similar accuracy, to estimate the dimensionless storage coefficient are based upon the pseudo time at which the radial flow ends before the transition period starts and the time of beginning of the second horizontal line:

$$\frac{1}{\omega} = 7.7534 + 2.8965\times10^{12}\left(\frac{\phi r_w^2}{kt_a(P)_{e1}}\right)^{1.5} \quad (49)$$

$$\omega = -9.0198\times10^{-3} + 2.5924x_2 - 80.1835x_2^2 + 3.5730\times10^{3}x_2^3 - 3.9119\times10^{4}x_2^4 \quad (50)$$

In this study, also a correlation for the interporosity flow parameter using the coordinates of the trough is developed. This is valid for $1x10^{-4} \le \lambda \le 1x10^{-8}$, with an error lower than 6% is reported:

$$\lambda = -2.5477\times10^{-10} + 4.1709x_5x_3 - 3.1769\times10^{7}(x_5x_3)^{2.5} + 6.4771\times10^{9}(x_5x_3)^3 - 2.5071\times10^{-26}\left(\frac{x_5}{x_3}\right)^2 \quad (51)$$

Another correlation using the point of intercept of the radial flow regime and the pseudosteady state transition flow with an error less than 3% is reported as:

$$\lambda = 8.5735\times10^{-12} + 5.4927x_5x_4 - 2.8230\times10^{5}(x_5x_4)^2 + 2.7210\times10^{8}(x_5x_4)^{2.5} - 4.8086\times10^{10}(x_5x_4)^3 \quad (52)$$

In order to estimate the skin factor, Eq. 5 is rewritten as:

$$s' = 0.5\left[\frac{\Delta m(P)_{r1}}{(t_a(P)*\Delta m(P)')_{r1}} - \ln\left(\frac{kt_a(P)_{r1}}{\omega\phi r_w^2}\right) + 7.43\right] \quad (53)$$

$$s' = 0.5\left[\frac{\Delta m(P)_{r2}}{(t_a(P)*\Delta m(P)')_{r2}} - \ln\left(\frac{kt_a(P)_{r2}}{\phi r_w^2}\right) + 7.43\right] \quad (53)$$

3. EXAMPLES

3.1 Synthetic example 1

Table reports the input data used to simulate a test for a fractured well inside a square-shaped gas reservoir. The model considers an infinite-conductivity fracture and results are shown in Figure-1. The purpose of this example is the determination of reservoir drainage area, reservoir permeability and half-fracture length.

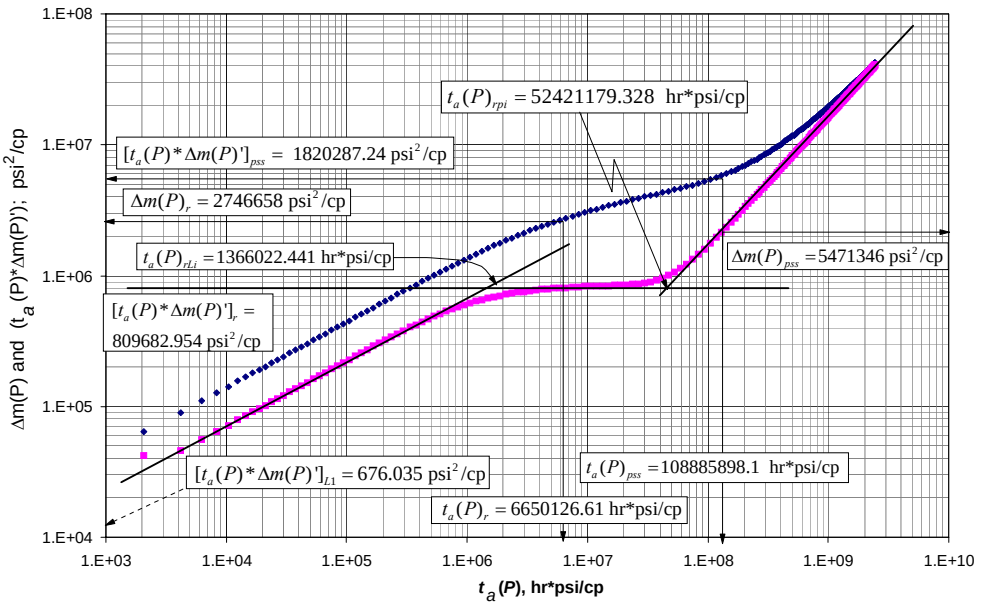

Figure-1. Pseudopressure and pseudopressure vs. pseudotime for example 1.

Solution

Three representative flow regimes are clearly seen in Figure-1. They are identified as early linear flow caused by the hydraulic fracture, then, followed by the radial flow regime and, finally, the late pseudoesteady-state period. The information listed below was read from Figure-1.

$t_a(P)_r$= 6650126.61 hr*psi/cp
$(t_a(P)*\Delta m(P)')_r$ = 809682.954 psi²/cp
$t_a(P)_{rpi}$= 52421179.328 hr*psi/cp
$t_a(P)_{rLi}$= 1366022.441 hr*psi/cp
$t_a(P)_{pss}$ = 108885898.1 hr*psi/cp
$\Delta m(P)'_r$ = 2746658 psi² /cp
$(t_a(P)*\Delta m(P)')_{pss}$= 1820287.24 psi²/cp
$(t_a(P)*\Delta m(P)')_{L1}$ = 676.035 psi²/cp
$\Delta m(P)')_{pss}$= 5471346 psi²/cp

Eqs. 9, 4, 11, 15, 5, 38 and 13 were employed to estimate the parameters provided in the third column of Table-1. The first row corresponds to Eq. 9, the second row to Eq. 4, and so on and so forth. Analogous expressions using rigorous time, Nunez *et al*. (2002), were used to estimate the same parameters as reported in column 4, Table-2.

Table-1. Well, gas and reservoir data for worked examples.

Parameter	Example 1	Example 2	Example 3	Example 5
q_{sc}, Mscf/D	2700	4000 and 1500	3000	6000
μ_{gi}, cp	0.022	0.022484	0.01961	0.03108
ϕ, %	23	19	10	20
h, ft	60	80	60	100
P_i, psia	3600	4000	5000	7000
T, ºR	694	760	660	710
r_w, ft	0.47	0.5	0.25	0.6
c_t, psi^{-1}	2.355x10^{-4}	2.08x10^{-4}	2.084 x10^{-4}	7.94536x10^{-5}
k , md	28	30	-	-
x_f, ft	380	100	-	-
$k_f w_f$, md-ft	-	10000	-	-
A, ft^2	21160000	-	-	-
λ	-	-	1x10^{-7}	-
ω	-	-	0.05	-

Table-2. Results for example 1.

Parameter	Value				
	Synthetic	From $t_a(P)$	From t, hr	EA $t_a(P)$ %	EA t %
x_f, ft	380	376.5	355.4	0.9	6.5
k, md	28	27.4	26.9	2	3.7
A, ft^2	21160000	19144121.5	18269868.4	9.5	13.6
A, f^2	21160000	20719791.6	18302811. 2	2.1	13.5
s'	-	-5.8	-5.8	-	-
x_e,ft	2300	2275.9	2151.8	1	6.4
C_A	-	56.8	40.7	-	-

3.2 Synthetic example 2

Figures 2 and 3 show simulated data on a reservoir having a square shape using the information from the third column of Table-1. The well model consists of a finite-conductivity fracture. The main purpose of this example is to compare the fracture conductivity obtained using pseudotime against the one obtained using rigorous time.

Solution

Bi-linear, radial and late-pseudosteady-state regimes are observed in Figures 2 and 3. The following information was read from Figure-2, for the case of q_{sc1} = 4000 MSCF/D:

$t_a(P)_r$= 186817873.9 hr*psi/cp $\quad \Delta m(P)'_r$ = 8692120.6 psi² /cp
$(t_a(P)*\Delta m(P)')_r$ = 921086.8422 psi²/cp $\quad (t_a(P)*\Delta m(P)')_{pss}$= 1820287.24 psi²/cp
$t_a(P)_{BD}$= 1062456.24 hr*psi/cp $\quad (t_a(P)*\Delta m(P)')_{BL1}$ =28708.815 psi²/cp

Also, the following information was read from Figure-3, for the case of q_{sc1} = 1500 MSCF/D:

$t_a(P)_r$= 199120292.7 hr*psi/cp $\quad \Delta m(P)'_r$ = 3283393 psi² /cp
$(t_a(P)*\Delta m(P)')_r$ = 343624.423 psi²/cp $\quad (t_a(P)*\Delta m(P)')_{pss}$= 1820287.24 psi²/cp
$t_a(P)_{BD}$=1062456.24 hr*psi/cp $\quad (t_a(P)*\Delta m(P)')_{BL1}$ =10720.767 psi²/cp

For both cases, Eqs. 4, 30 and 39 were used to estimate permeability, apparent fracture conductivity and apparent half-fracture length. Equations for the same purpose using rigorous time were taken from Nunez *et al*. (2003) to compare the results. All the results are reported in Tables 3 and 4. From Eq. 29, the dimensionless fracture conductivity is 2.8. Following the procedure described by Guppy *et al*. (1081), an *a* value of 0.964 is found with Eq. 31. Then, the total dimensionless fracture conductivity, Eq. 32, is 2.865.

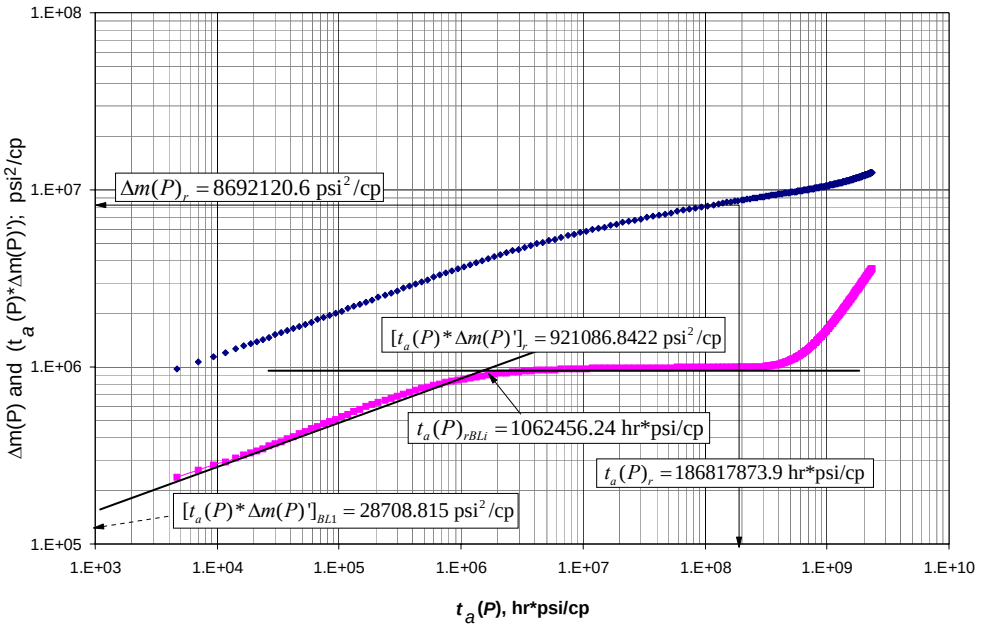

Figure-2. Pseudopressure and pseudopressure vs. pseudotime for example 2, q_{sc} = 4000 Mscf/D.

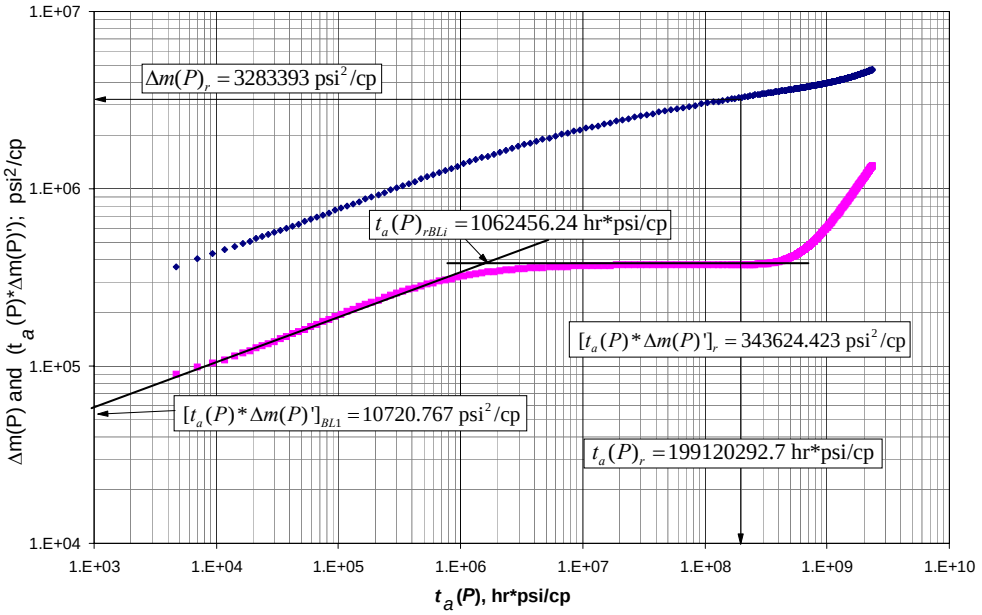

Figure-3. Pseudopressure and pseudopressure vs. pseudotime for example 2, q_{sc} = 1500 Mscf/D.

Table-3. Results for example 2, $q_{sc1.}$

Parameter	Value				
	Synthetic	**From $t_a(P)$**	**From t**	**EA $t_a(P)$ %**	**EA t %**
x_f, ft	100	116.91552	132.56092	16.91552	32.560924
k, md	30	29.343466	28.491331	2.1884482	5.0288951
$k_f w_f$, md-ft	10000	9154.5416	8770.9429	8.4545838	12.290571

Table-4. Results for example 2, q_{sc2}.

Parameter	Value				
	Synthetic	From $t_a(P)$	From t	EA $t_a(P)$ %	EA t %
x_f, ft	100	112.2457	128.02485	12.245697	28.024852
k, md	30	29.495735	28.590709	1.6808826	4.6976358
$k_f w_f$, md-ft	10000	9207.7612	8993.9126	7.9223883	10.060874

Notice that in this example the late pseudosteady-state period was not used since that case was already considered by Escobar *et al*. (2997) and treated in example 1.

3.3 Example 3

Figure-4 contains the pseudopressure and pseudopressure derivative vs. pseudotime data of a hydraulic fractured gas well presented by Lee and Wattanberger (1996), which relevant information is given in the fourth column of Table-1. It is requested to determine reservoir permeability and half-fracture length.

Solution

In the log-log plot of Figure-4, the linear flow regime is clearly seen to dominate the early time data. This period is followed by a bi-radial flow period (although not used in this example), then, a shot radial flow regime and a well defined pseudosteady-state regime. From this plot the following data are read:

$t_a(P)_r$= 22067058.58 hr*psi/cp $\quad \Delta m(P')_r$ =500380871.6376 psi²/cp

$(t_a(P)*\Delta m(P')_r$ =245000000 psi²/cp $\quad (t_a(P)*\Delta m(P')_{BL1}$= 1820287.24 psi²/cp

$(t_a(P)*\Delta m(P')_{L1}$ =89340.6177 psi²/cp

Permeability, skin factor and half-fracture length are calculated using Eqs. 4, 5 and 9, respectively. Similar expressions using rigorous time, as reported by Nunez *et al*. (2002), were used to estimate the same parameters. All the results are given in Table-4.

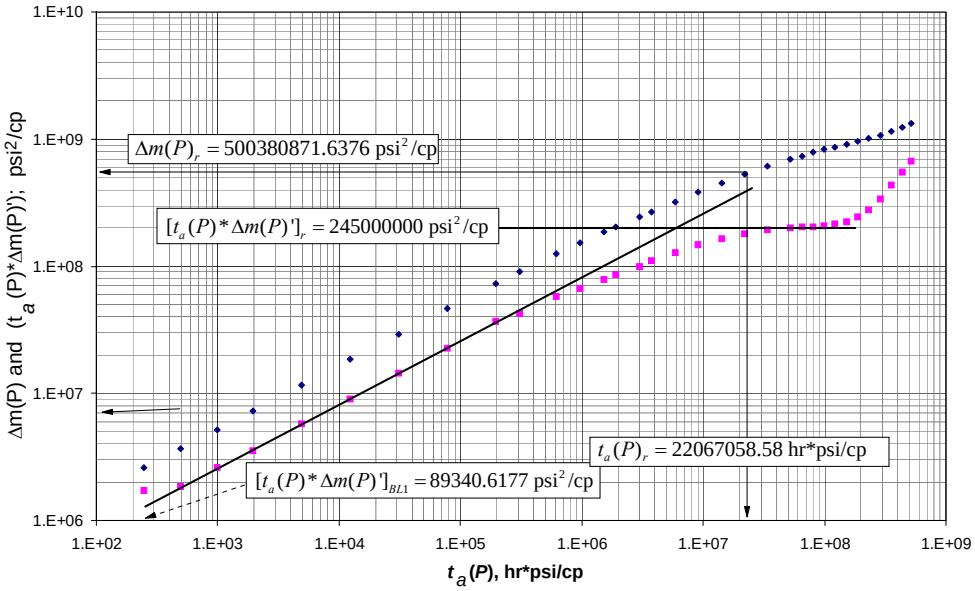

Figure-4. Pseudopressure and pseudopressure vs. pseudotime for example 3.

Table-4. Results for example 3.

Parameter	Value				
	Actual*	From $t_a(P)$	From t	EA $t_a(P)$ %	EA t %
x_f, ft	77	77.25	77.9	0.003246753	0.0116883
k, md	0.088	0.095	0.075	0.079545455	0.1477273
s'	-4.94	-5.083	-5.11	0.028947368	0.034413

(*) Data obtained from a commercial simulator

3.4 Synthetic example 4

A pressure test for a double-porosity system was performed using the data from the fifth column of Table-1. The model assumed neither wellbore storage nor skin factor. The purpose of this example is to obtain the interporosity flow parameter and the dimensionless storage coefficient.

Solution

Figure-5 shows the pseudopressure and pseudropressure derivative log-log plot. The typical "v" shape confirms the presence of a double-porosity system. From that plot the following information is read:

$t_a(P)_r$= 951178425.3987 hr*psi/cp
$\Delta m(P')_r$ = 12629134.3667 psi² /cp
$(t_a(P)*\Delta m(P)')_r$ = 637082.6886 psi²/cp
$(t_a(P)*\Delta m(P)')_{el}$= 57669.5743 psi²/cp
$t_a(P)_{min}$= 8389609.9968 hr*psi/cp
$(t_a(P)*\Delta m(P)')_{rb2}$ = 319645590.3 psi²/cp
$t_a(P)_{us}$= 60216581.0339 hr*psi/cp
$(t_a(P)*\Delta m(P)')_{min}$ = 132739.7325 hr*psi/cp

Eq. 4 allows the estimation of a permeability value of 47.56 md and Eq. 53 is used to estimate a skin value of 0.0435. Eqs. 48, 49 and 50 were used to estimate ω and Eqs. 51 and 52 were used to obtain values ofλ. The results are given in Table-5 along with results from similar correlations for rigorous time as presented by Escobar *et al*. (2004).

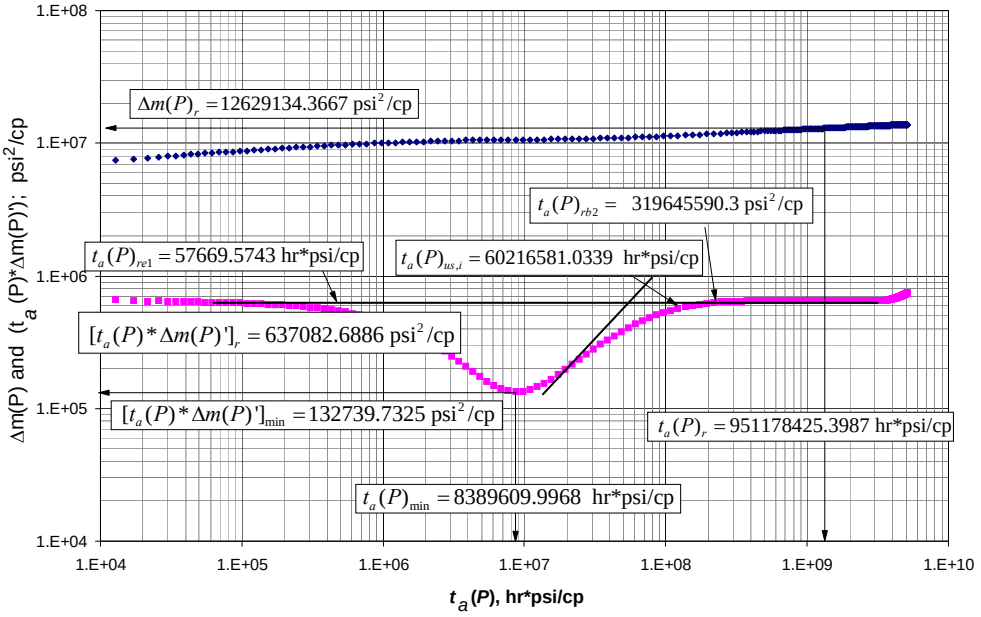

Figure-5. Pseudopressure and pseudopressure vs. pseudotime for example 4.

Table-5. Results of example 4.

Parameter	Value				
	Synthetic	From $t_a(P)$	From t	EA $t_a(P)$ %	EA t %
ω	0.05	0.04978398	0.0543965	0.43204	8.79314
ω	0.05	0.04981871	0.0474290	0.36258	5.14192
ω	0.05	0.04982332	0.0539870	0.35336	7.97402
λ	$1x10^{-7}$	$1.11x10^{-7}$	$1.11x10^{-7}$	11.24	11.37
λ	$1x10^{-7}$	$9.81x10^{-8}$	$1.02x10^{-7}$	1.853	2.33
k, md	50	47.5600366	47.460112	4.879926	5.079775
s'	0	0.04354457	0.13509576	4.354457	13.50957

3.5 Example 5

A pressure test was run in a gas well located in a Colombian reservoir. Pseudopressure and pseudopressure derivative vs. pseudotime data are plotted in Figure-6. Gas, well and reservoir properties are given in the sixth column of Table-1. It is required to determine reservoir permeability and the double-porosity reservoir parameters.

Solution

The following information was read from Figure-6.

$t_a(P)_r$= 138811698.8 hr*psi/cp
$\Delta m(P')_r$ = 252325291.8877 psi² /cp
$(t_a(P)*\Delta m(P')_r$ = 1263040.9589 psi²/cp
$(t_a(P)*\Delta m(P')_{e1}$= 58037.4 psi²/cp
$t_a(P)_{min}$= 1063339.1063 hr*psi/cp
$(t_a(P)*\Delta m(P')_{b2}$ = 25945471.29 psi²/cp
$t_a(P)_{us,i}$= 6030597.57 hr*psi/cp
$(t_a(P)*\Delta m(P')_{min}$ = 398453.8087 hr*psi/cp

As for example 4, same relationships were used in similar order. The results are provided in Table-6.

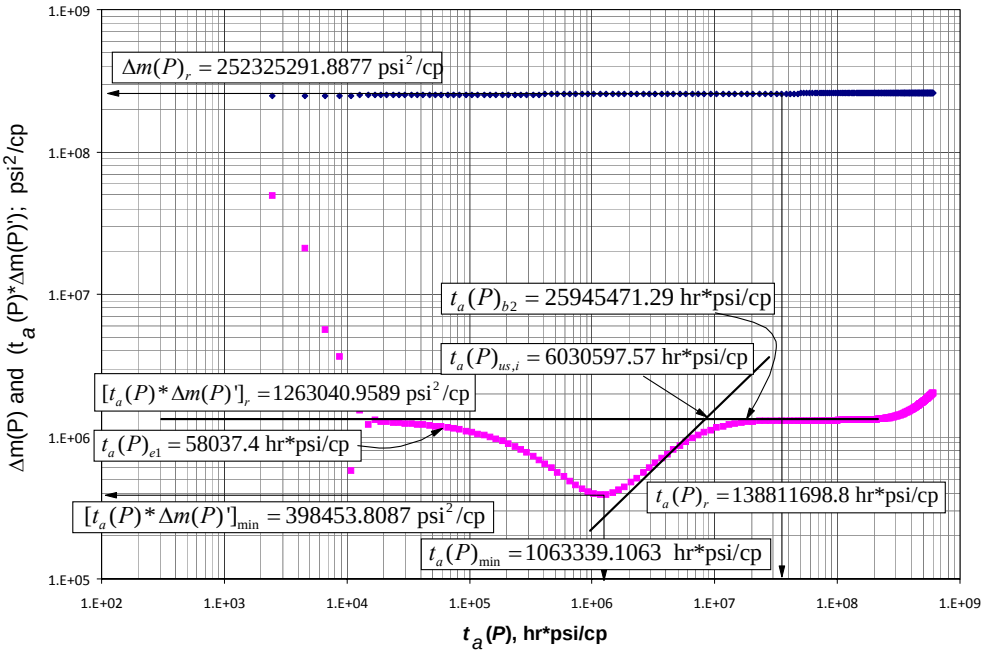

Figure-6. Pseudopressure and pseudopressure vs. pseudotime for example 5.

Table-6. Results of example 5.

Parameter	PRUEBA 5				
	Actual*	**From $t_a(P)$**	**From t**	**EA $t_a(P)$ %**	**EA t %**
ω	0.0998	0.09463	0.09295	5.17	6.86
ω	0.0998	-	-	-	-
ω	0.0998	0.09814	0.03216	1.66	67.7
λ	$1.1x10^{-6}$	$5.63\ x10^{-7}$	$6.49\ x10^{-7}$	48.8	40.95
λ	$1.1x10^{-6}$	$4.48\ x10^{-7}$	$4.053\ x10^{-9}$	59.26	63.15
k, md	20	19.0057	18.6027	4.9713	6.9863
s'	90	90.55	86.59	0.613	3.78

(*) Data obtained from a commercial simulator

4. ANALYSIS OF RESULTS

In this work, we found that using pseudotime instead of rigorous or actual time leads to less deviation errors of some of the important parameters obtained from gas pressure well tests. Escobar *et al*. (2007) found an impact on reservoir drainage area estimation; see Table-2, but less effect on reservoir permeability and skin factor as seen in Tables 2 through 6. In example 2 and 3 the deviation on the estimation of the fracture conductivity is reduced when using pseudotime. In example 4 the estimation of the half-fracture length is much better when using pseudotime. In example 4 and 5 the estimation of ω and λ has also a significant lower deviation error when estimated with pseudotime. It is also confirmed from example 1 that the reservoir drainage area is better

estimated using pseudotime instead of real time as presented by Escobar *et al*. (2007).

Nomenclature

A	Reservoir drainage area, ft^2
C_A	Dietz's shape factor
C_{fD}	Dimensionless fracture conductivity
D	Non-Darcy flow coefficient, $(Mscf/D)^{-1}$
c_t	Compressibility, 1/psi
h	Formation thickness, ft
k	Permeability, md
$k_f w_f$	Fracture conductivity, md-ft
m(P)	Pseudopressure function, psi^2/cp
P	Pressure, psi
q_{sc}	Gas flow rate, Mscf/D
r_w	Well radius, ft
s	Skin factor
s'	Pseudoskin factor
T	Temperature, °R
t	Time, hr
$t_a(P)$	Pseudotime function, psi hr/cp
$t_a(P)*\Delta m(P)'$	Pseudopressure derivative function, psi^2/cp
t_{Da}	Dimensionless pseudotime with respect to r_w
t_{DaA}	Dimensionless pseudotime with respect to A
t_{Daxf}	Dimensionless pseudotime with respect to x_f
x_e	Reservoir half length, ft
x_f	Half-fracture length, ft
x_1	$[t_a(P)*\Delta m(P)']_{min}/[t_a(P)*\Delta m(P)']_r$
x_2	$[t_a(P)]_{min}/[t_a(P)']_{rb2}$
x_3	$[t_a(P)*\Delta m(P)']_{min}/[t_a(P)]_{min}$
x_4	$[t_a(P)*\Delta m(P)']_{us,i}/[t_a(P)]_{us,i}$
x_5	$h\phi r_w^2/q_{sc}T$
Z	Gas deviation factor

Greek

Δ	Change, drop
ϕ	Porosity, fraction
μ	Viscosity, cp
λ	Interporosity flow parameter
ω	Dimensionless storativity coefficient

Subscripts

app1	Apparent for the first flow rate
app2	Apparent for the second flow rate
BR1	Bi-radial at pseudotime of 1 psi*hr/cp
BRpi	Intersect of bi-radial and pseudosteady-state lines
BRLi	Intersect of bi-radial and linear lines
BLLi	Bilinear and linear intersection
BL1	Bilinear at pseudotime of 1 psi*hr/cp
D	Dimensionless
b_2	Start of first radial flow
e_1	End of first radial flow
f+m	Total = matrix plus fracture
g	Gas
i	Intersection or initial conditions
L	Linear
L1	Linear flow at pseudotime of 1 psi*hr/cp
Lpi	Intersect of linear and pseudosteady-state lines
min	Minimum
p, pss	Pseudosteady state
r	radial flow
r_1	Radial flow before the transition in a double-porosity system
r_2	Radial flow after the transition in a double-porosity system
rBLi	Intersection of radial and bilinear flow regimes
rBRi	Intersection of radial and bi-radial flow regimes
rLi	Intersection of radial and linear flow regimes
rpi	Intersection of radial and pseudosteady-state lines
sc	Standard conditions
us,i	Intercept of the transition unit-slope line with the radial flow line
w	Well

Abbreviations

EA $t_a(P)$ %	Absolute error with respect to peudotime, percent
EA $t_a(P)$ %	Absolute error with respect to rigorous time, percent
Eq.	Equation
Eqs.	Equations
Fig.	Figure
Figs.	Figures

5. CONCLUSIONS

New expressions to characterize gas reservoir with the *TDS* technique for fractured vertical wells and double-porosity systems were introduced. The results of the new developed equations were compared to the results obtained when using actual time. Better results of fracture half-length, fracture conductivity, dimensionless storage coefficient and interporosity flow parameter are obtained when using pseudotime than rigorous time. In some cases the deviation error was reduced more than one half.

ACKNOWLEDGMENTS

The authors gratefully thank Universidad Surcolombiana and Ecopetrol-ICP for providing support for the completion of this work.

REFERENCES

Agarwal G. 1979. Real Gas Pseudo-time a New Function for Pressure Buildup Analysis of MHF Gas Wells. Paper SPE 8279 presented at the 54th technical conference and exhibition of the Society of Petroleum Engineers of AIME held in Las Vegas, NV, Sep. 23-26.

Al-Hussainy R., Ramey H. J. Jr. and Crawford P.B. 1966. The Flow of Real Gases Through Porous Media. J. Pet. Tech. 624-636; trans., AIME, p. 237.

Cinco-Ley H., Samaniego F. and Dominguez N. 1976. Transient Pressure Behavior for a Well with a Finity-Conductivity Vertical Fracture. Paper SPE 6014 presented at the SPE-AIME 51st Annual Fall Technical Conference and Exhibition, held in New Orleans, LA, Oct. pp. 3-6.

Engler T. and Tiab D. 1996. Analysis of Pressure and Pressure Derivative without Type Curve Matching, 4. Naturally Fractured Reservoirs. Journal of Petroleum Science and Engineering. 15: 127-138.

Escobar F.H., Carvajal J.M., Ramirez J.P. and Y. Medina O.I. 2004. Análisis de Presión y Derivada de Presión para Yacimientos de Gas Naturalmente Fracturados Drenados por un Pozo Vertical. Revista Entornos N° 18, December. pp. 30-45.

Escobar F.H., López A.M. and Cantillo J.H. 2007. Effect of the Pseudotime Function on Gas Reservoir Drainage Area Determination. CT&F - Ciencia, Tecnologíay Futuro. 3(3): 113-124, December.

Guppy K.H., Cinco-Ley H. and Ramey H.J. Jr. 1981. Pressure Buildup Analysis of Fractured Wells Producing at High Flow Rates. Paper SPE 10178.

Lee W. J. and Holditch S. A. 1982. Application of Pseudotime to Buildup Test Analysis of Low-Permeability Gas Wells with Long-Duration Wellbore Storage Distortion. J. Pet. Tech. pp. 2877-2887, December.

Lee J. and Wattenbarger R.A. 1996. Gas Reservoir Engineering. SPE Textbook Series. Vol. 5.

Nunez W., Tiab D. and Escobar F. H. 2002. Análisis de Presiones de Pozos Gasíferos verticales con Fracturas de Conductividad Infinita en Sistemas Cerrados Sin Emplear Curvas Tipo. Boletín Estadístico Mensual del ACIPET. No. 4, Year 35, ISSN 0122 5728. pp. 9-14. October.

Nunez W., Tiab D. and Escobar F.H. 2003. Transient Pressure Analysis for a Vertical Gas Well Intersected by a Finite-Conductivity Fracture. Paper SPE 80915, Proceedings, prepared for presentation at the SPE Production and Operations Symposium held in Oklahoma City, Oklahoma, U.S.A. pp. 23-25, March.

Spivey J. P. and Lee W. J. 1986. The Use of Pseudotime: Wellbore Storage and the Middle Time Region. Paper SPE 15229 presented at the Unconventional Gas Technology Symposium of the SPE held in Louisville, Kentucky, USA, from 18-21 May.

Tiab D. 1993. Analysis of Pressure and Pressure Derivative without Type-Curve Matching: 1- Skin Factor and Wellbore Storage. Paper SPE 25423 presented at the Production Operations Symposium held in Oklahoma City, USA, Mar. 21-23. pp. 203-216. Also published in Journal of Petroleum Science and Engineering. 12(1995): 171-181.

Tiab D. 1994. Analysis of Pressure Derivative without Type-Curve Matching: Vertically Fractured Wells in Closed Systems. Journal of Petroleum Science and Engineering. 11: 323-333.

Tiab D. and Escobar F.H. 2003. Determinación del parámetro de flujo interporoso por medio de un gráfico semilogarítmico. X Colombian Petroleum Symposium.

Tiab D. 2003. Advances in pressure transient analysis-TDS Technique. Lecture Notes Manual. The University of Oklahoma, Norman, Oklahoma, USA. p. 577.